

A NEW EQUATION FOR THE SUCTION INDUCED SHRINKAGE OF CLAYEY SOILS

Mamert Mbonimpa*, Université du Québec en Abitibi-Témiscamingue, Rouyn-Noranda, Québec, Canada.

Michel Aubertin, École Polytechnique de Montréal, Montréal, Québec, Canada.

Bruno Bussière, Université du Québec en Abitibi-Témiscamingue, Rouyn-Noranda, Québec, Canada.

Abdelkabar Maqsooud, Université du Québec en Abitibi-Témiscamingue, Rouyn-Noranda, Québec, Canada.

*Corresponding Author: mamert.mbonimpa@uqat.ca

ABSTRACT

An increase of the suction applied to a deformable soil may induce shrinkage and desaturation. This makes the determination of the water retention curve (WRC) of such soils more complex, as one needs to follow simultaneously the volumetric shrinkage curve (VSC) and the water content. Descriptive and predictive models can be useful to assess the behaviour of compressible soils. After reviewing typical results obtained on relatively soft and initially saturated clayey soils, the authors introduce new equations to describe the VSC. A simplified tree linear segment representation, inspired by the consolidation theory, is first used. It is then generalised using a curvilinear equation. The proposed models describe the VSC in terms of the change of void ratio e with an increase in suction ψ . Experimental data are used to validate the descriptive capabilities of the VSC models. For predictive purposes, empirical relationships are proposed to estimate the model parameters from the liquid and plastic limits, solid grain density, and initial void ratio. The typical results shown here indicate a good agreement between measured and calculated VSC.

RÉSUMÉ

Une augmentation de la succion appliquée à un sol déformable induit un retrait et une désaturation. La détermination de la courbe de rétention d'eau (CRE) de tels sols devient complexe car il faut en même temps connaître la courbe de retrait volumique (CRV). Des modèles descriptifs et prédictifs peuvent être utiles pour évaluer le comportement de sols compressibles. Suite à une analyse de résultats typiques obtenus sur des sols argileux relativement mous, initialement saturés, les auteurs présentent des équations descriptives de la CRV. Une description simplifiée de la CRV par trois segments linéaires inspirée de la théorie de consolidation est d'abord utilisée. Elle est ensuite généralisée en utilisant une représentation curvilinéaire. Les modèles proposés décrivent la CRV en termes de réduction de l'indice des vides e avec l'augmentation de la succion ψ . Des données expérimentales sont utilisées pour valider la capacité de ces modèles à décrire la CRV. Pour des fins de prédiction, des relations empiriques sont proposées pour estimer les paramètres des modèles à partir des limites de liquidité et de plasticité, de la densité des particules solides et de l'indice des vides initial. Les résultats types montrés ici indiquent une bonne concordance entre les CRV mesurées et calculées.

1. INTRODUCTION

Measurement approaches of the water retention curve (WRC) for incompressible soils are based on the determination of gravimetric (w) or volumetric (θ) water content at given suction values (ψ), on sample(s) submitted to drying or wetting processes, generally for constant zero total stress. These measurements use different techniques, described in literature (e.g., Fredlund and Rahardjo 1993; Aubertin et al. 1997; Barbour 1998; Delleur 1998; Delage and Cui, 2000a; Wilson et al. 2000). For such soils, the void ratio (e) remains constant during the drying and/or wetting processes. The degree of saturation (S_r) associated to measured w or θ can then be easily derived for different suction values ψ using eq. 1, where D_r is the specific gravity of the solid particle.

$$[1] \quad \theta = \frac{e}{1+e} S_r = \frac{D_r}{1+e} w$$

In the case of compressible (shrinking) soils, a suction increase may induce desaturation (i.e. reduction of S_r) and volume change simultaneously. Experimental procedures to obtain the WRC must thus involve the measurement of the water content and of the total specimen volume, for the suction increments. The soil volume change can be determined by applying displacement methods based on immersion of the specimen in a mercury filled cup (e.g., ASTM D427-98; Silvestri 1994), or in water after the specimen surface has been sealed with a wax (ASTM D4943-95), or in toluene (Sibley and Williams 1989). Other types of measurements of the volume change can also be performed using alternative techniques, including suction controlled oedometers (Fredlund and Rahardjo 1993; Cabral et al. 2004) and retractometers (Braudeau et al. 1999; Geiser et al. 2000). The volume change due to shrinkage can be represented with different parameters such as the void ratio e (e.g. Biarez et al. 1987; Delage and Cui, 2000a), the specific volume (volume of the sample/masse of the oven dry sample; e.g., Braudeau et al. 1999; Crescimanno and Provenzano 1999; Chertkov

2000, 2003; Tripathy et al. 2002), or other related material characteristics. The plot of the volume change against water content or against suction is usually designated as the volumetric shrinkage curve (VSC), although other terms are also sometimes used to describe such relationships.

A typical VSC defined schematically with the function $e-w$ is illustrated in Figure 1a (inspired by Biarez et al. 1987; Konrad and Ayad 1997; Tripathy et al. 2002; Chertkov 2000, 2003; Braudeau and Mohtar 2004). The corresponding VSC defined in the $e-\log \psi$ plane is shown in Fig. 1b. The related water retention curve(s) expressed using the $w-\log \psi$, $\theta-\log \psi$, and $S_r-\log \psi$ relationships are shown in Fig. 1c.

Three shrinkage phases can generally be distinguished on a typical VSC drawn from saturation to full dryness, without external stress applied. These are: Phase 1 (normal) corresponding to saturated shrinkage; Phase 2 (residual) which combines desaturation and shrinkage; Phase 3 (no-shrinkage) where the volume is considered quasi constant (e.g., Haines 1923; Marshall et al. 1996; Braudeau et al. 1999, Braudeau and Mohtar 2004).

In the normal shrinkage zone (Phase 1), the volume change equals the volume of water lost, so that the soil remains saturated (i.e. drainage follows the saturation line). The transition between Phases 1 and 2 occurs at the water content w_a corresponding to the air entry value AEV (ψ_a), when air enters the voids. In the residual zone (Phase 2), the volume decrease is smaller than the volume of water loss. This desaturation increases the resistance of the soil to deformation (e.g. Delage and Cui, 2000b). The transition between Phases 2 and 3 occurs at the “true” shrinkage limit w_{es} . In Phase 3, particles are under maximum contact and further volume change is considered negligible (the void ratio is almost constant, with $e = e_s$); nonetheless, the water content (and degree of saturation) can further diminish until complete dryness.

According to Haines (1923) and Marshall et al. (1996), ψ_a of compressible clayey soils is typically around 10^5 cm (i.e. negative pressure close to 10^4 kPa), while the shrinkage limit w_{es} is reached at a suction (head) ψ_{es} of about 10^6 cm. The suction corresponding to complete dryness takes a value close to 10^7 cm (Ross et al., 1991; Fredlund and Xing, 1994). In geotechnical practice, the shrinkage limit w_s (%) is typically defined on the saturation line as shown on Fig. 1a; it corresponds to the saturated water content associated to e_s ($e_s = D_r w_s / 100 = D_r w_{es} / 100 S_{r,es}$, where $S_{r,es}$ is the degree of saturation at the onset of the no-shrinkage phase).

It is worth mentioning that the shrinkage path for initially unsaturated materials can be different from that of saturated soils (e.g., Tripathy 2002, Braudeau and Mohtar 2004). This added level of complexity will not be addressed here. Furthermore, in surface soils with an aggregated structure and dual porosity, an initial phase (called structural shrinkage) may be observed before

Phase 1 (e.g., Tripathy et al. 2002; Chertkov 2000, 2003; Braudeau and Mohtar 2004). In this phase, a few large pores are easily drained, and the decrease in soil volume is less than the volume of water lost as air enters these voids. Only the 3 phases identified in Fig. 1 will be considered in this study.

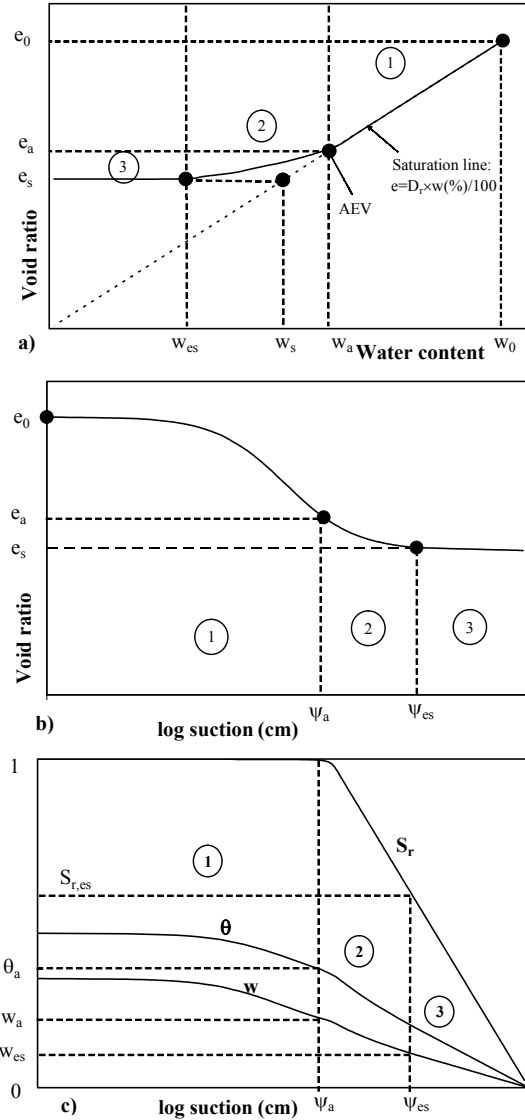


Fig 1. Schematic illustration of the shrinkage and desaturation phases of a compressible soil, shown in various planes: **a)** $e-w$; **b)** $e-\log \psi$; **c)** WRC expressed as $w-\log \psi$, $\theta-\log \psi$ and $S_r-\log \psi$ (Adapted from Mbonimpa et al. 2005).

As illustrated by Fig. 1, the WRC measurement is more complicated for deformable materials than for incompressible as the VSC determination is also involved. In this regard, predictive models may be useful tools, especially at the preliminary stage of a project when an estimate of the soil response can provide insights on the expected results. For that purpose, the

authors have extended the modified Kovács model developed to predict WRC of stiff soils (Aubertin et al. 2003) to shrinking clayey soils (Mbonimpa et al. 2005). The extended MK model uses the function $e(\psi)$. It is thus helpful to have means to estimate, in a simple and practical manner, the relationship between e and ψ of compressible soil. This paper introduces simple linear and non-linear models to describe, and in some cases to predict, the VSC (e - $\log\psi$) of compressible materials. The proposed model parameters are first obtained by fitting calculated VSC to experimental data taken from the literature. For the predictive applications, these parameters are related to basic geotechnical properties. The proposed predictive approach is evaluated by comparing predicted values to measured data. The paper ends with a short discussion and conclusion.

2. PROPOSED VSC EQUATIONS

2.1 Soils considered in this study

The data needed for the present study are those for which the tests were performed on relatively soft soils samples under drainage conditions (from $S_r = 100\%$), and for which the basic geotechnical parameters were given. These parameters are required for predictive applications. The data used here are taken from the SOILVISION database (Fredlund 1999), from Biarez et al. (1987) and from Fleureau et al. (1993, 2002). The data are identified in Table 1; D_r is the relative density of the solid particles, w_L is the liquid limit, w_P is the plastic limit, w_s is the shrinkage limit; e_0 is the initial void ratio, and e_s is the final void ratio on the $e(\psi)$ curve. The shrinkage limit w_s has been obtained from the curve $e(w)$ using the plot shown in Figure 1a. SOILVISION includes information on $e(w)$ and $w(\psi)$; the $e(\psi)$ curves have then been inferred from these relationships. For the data taken from Fleureau et al. (1993, 2002) and Biarez et al. (1987), the values of $e(w)$ and $e(\psi)$ were obtained by digitizing the published figures.

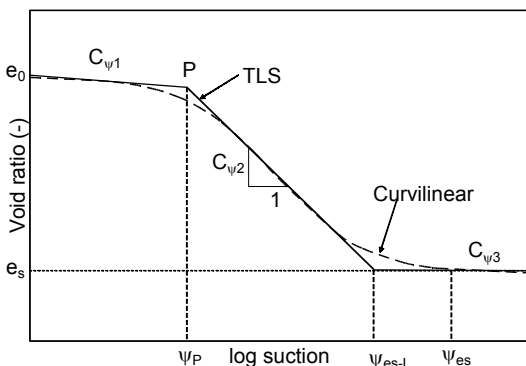


Fig. 2. Description of the e - $\log\psi$ curve using three linear segments (TLS) and a curvilinear representation

Experimental results show that the typical VSC, represented by a e - $\log\psi$ relationship, has an S shape that can be described with three linear segments (TLS)

or with an appropriate curvilinear equation (see Fig. 2). The former representation makes physical interpretation easier while the latter better reflects the reality of a continuous transition along the shrinkage path.

2.2 VSC description with three linear segments

This representation is inspired from an idealized consolidation curve. The void ratio first decreases from its initial value e_0 to e_P (at a suction ψ_P) associated to the transition point P. The corresponding slope $C_{\psi 1}$ is typically very small. Beyond e_P , shrinkage is more pronounced and it reduces the void ratio until it reaches e_s associated to the end of the residual shrinkage phase, following the slope $C_{\psi 2}$. With this linear model, the onset of the no-shrinkage phase appears to occur at suction ψ_{es-L} , which is lower than the actual suction ψ_{es} defined in Fig. 1b. The last stage brings e_s to the final void ratio along slope $C_{\psi 3}$ (which is again very small). For practical applications, it will be assumed that $e(\psi) = e_0$ for $0 \leq \psi \leq \psi_P$ and $e(\psi) = e_s$ for $\psi \geq \psi_s$, i.e. $C_{\psi 1} = C_{\psi 3} = 0$. The VSC for $\psi_P \leq \psi \leq \psi_s$ follows the slope $C_{\psi} \equiv C_{\psi 2}$, and it can be defined as:

$$[2] \quad e(\psi) = e_0 - C_{\psi} \log\left(\frac{\psi}{\psi_P}\right) = e_s + C_{\psi} \log\left(\frac{\psi_{es-L}}{\psi}\right)$$

with

$$[3] \quad C_{\psi} = -\frac{de}{d\log(\psi)} = \frac{(e_0 - e_s)}{\log\left(\frac{\psi_{es-L}}{\psi_P}\right)}$$

2.3 VSC description with continuous function

Various curvilinear continuous mathematical expressions (similar to those used to describe the WRC for instance) can be used to describe the VSC. Functions with the minimum adjustable parameters have been targeted here. The authors investigations indicate that a good agreement between measured and calculated values of $e(\psi)$ can be obtained with the following equation:

$$[4] \quad e(\psi) = e_s + \frac{e_0 - e_s}{1 + \alpha \psi^{\beta}}$$

where α and β are model parameters. Parameter α controls the position at the onset of a significant void ratio decrease (equivalent to point P) while parameter β affects the slope of the VSC. This mathematical formulation has been inspired by the Gardner (1956) equation for the WRC.

3. APPLICATION OF THE VSC MODELS

In the following paragraph, the models are used to describe experimental results. Predictive applications follows with parameter values deduced from basic geotechnical properties.

Table 1. Samples characteristics and fitted parameters used in this study.

Sample ¹	Record or soil	G _s (-)	w _L (%)	w _P (%)	w _s (%)	e ₀ (-)	e _s (-)	ψ _p (cm)	ψ _{es-L} (cm)	C _ψ (-)	α (-)	β (-)
1	6042	2.67	78	26	17	0.887	0.460	94	40272	0.162	0.001	0.853
2	6044	2.65	60	27	22	0.838	0.580	32	31435	0.086	0.005	0.751
3	6061	2.64	40	27	18	0.950	0.470	38	24000	0.171	0.002	0.802
4	6065	2.70	75	24	16	0.855	0.411	500	231013	0.167	0.0001	0.940
5	6066	2.83	80	33	20	2.690	0.511	7	100000	0.524	0.028	0.519
6	6068	2.73	51	16	13	1.755	0.370	7	14000	0.419	0.026	0.661
7	6069	2.80	92	26	16	3.000	0.510	9	100000	0.615	0.027	0.621
8	6072	2.69	71	24	16	2.488	0.510	7	13000	0.605	0.035	0.612
9	6073	2.73	64	31	22	2.147	0.593	20	15000	0.540	0.010	0.754
10	6079	2.84	70	38	16	2.390	0.412	10	150000	0.474	0.027	0.527
11	6080	2.77	58	33	26	2.153	0.690	2	7000	0.413	0.059	0.643
12	FoCa clay	2.68	90	35	17	3.632	0.511	3	124097	0.676	0.039	0.501
13	Jossigny loam	2.74	37	18	15	1.268	0.435	9	26300	0.240	0.012	0.716
14	White clay	2.65	60	30	32	1.980	0.850	80	30000	0.439	0.002	0.875
15	Kaolinite	2.65	61	30	29	2.149	0.830	10	27000	0.384	0.006	0.691
16	Loam	2.70	27	20	22	0.798	0.600	4	5170	0.064	0.008	0.948
17	Marl	2.75	36	23	15	1.078	0.430	4	20000	0.175	0.022	0.639

¹Data for samples 1 to 11 are taken from SOILVISION (Fredlund 1999); data for samples 12 to 14 taken from Fleureau et al. (1993, 2002); data for samples 15 to 17 taken from Biarez et al. (1987).

3.1 Descriptive application

Figure 3 shows typical measured data, in the e-logψ plane, with fitted curves. These results have been obtained by using the simplified TLS model (eq. 2 – assuming C_{ψ1} = C_{ψ3} = 0) and the non linear equation (eq. 4). The fitting procedure has been performed with a graphical method for the TSL model, and by minimizing the sum of the squares of the residuals using the solver of Microsoft Excel[®] for the curvilinear equation. In all cases, e_s values obtained graphically on the e(ψ) curves were considered. It can be observed that the assumption C_{ψ1} = C_{ψ3} = 0 is in close agreement with the experimental results. The fitted parameters (ψ_p, ψ_{es-L} and C_ψ for the TLS model and α and β for the curvilinear equation) are given in Table 1. The value for ψ_{es-L} is mostly comprised between 10⁴ cm and 10⁵ cm. Actual suction values ψ_{es} are comprised between 10⁵ cm and 10⁶ cm, close to the expected value as defined above by Haines (1923; see also Marshall et al., 1996). On the other hand, the values for ψ_p are typically smaller than 100 cm, except for Sample 4 (500 cm). It should be mentioned that the position of the transition points (P and S) on the TLS representation are somewhat subjective, and as a semi-log scale is used, a slight difference can lead to a significant variation of ψ_p and ψ_{es-L} (an optimisation procedure could help minimize this uncertainty). The slope C_ψ varies between 0.06 and 0.7. With the non linear equation, it has been observed that 0.0001 ≤ α ≤ 0.06 and 0.5 ≤ β ≤ 1.0. The value of α is inversely proportional to ψ_p (results not shown here).

3.2 Predictive application

Investigations have been conducted to use the VSC equations for predictive applications. For that purpose, the model parameters have been estimated using

empirical correlations based on commonly used geotechnical properties.

- Parameters e_s

The void ratio e_s is related to the shrinkage limit w_s determined using e(w) data obtained by performing shrinkage limit tests (e.g. ASTM D 427-98, ASTM D 4943-02). It is recognized however that the experimental determination of w_s is not always very accurate (Holtz and Kovacs 1981). A practical alternative is to estimate w_s. This parameter can be obtained indirectly from the well known Plasticity Chart using the A and U lines and an empirical graphical method proposed by Casagrande (in Holtz and Kovacs 1981). A more representative correlation was established by the authors based on the linear relationship between the shrinkage index I_s (= w_L - w_s) and the plasticity index I_p (= w_L - w_P); this correlation is shown in Figure 4. The shrinkage limit w_s can hence be estimated (for w_L ≤ 5.6 w_P approximately) as:

$$[5] \quad w_s = w_L - 1.22 I_p$$

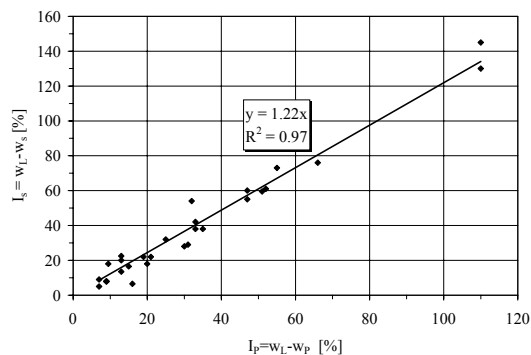


Fig.4. Relationship between the shrinkage index I_s and the plasticity index I_p (using data from Table 1, and additional data taken from Fleureau et al. 1993, 2002)

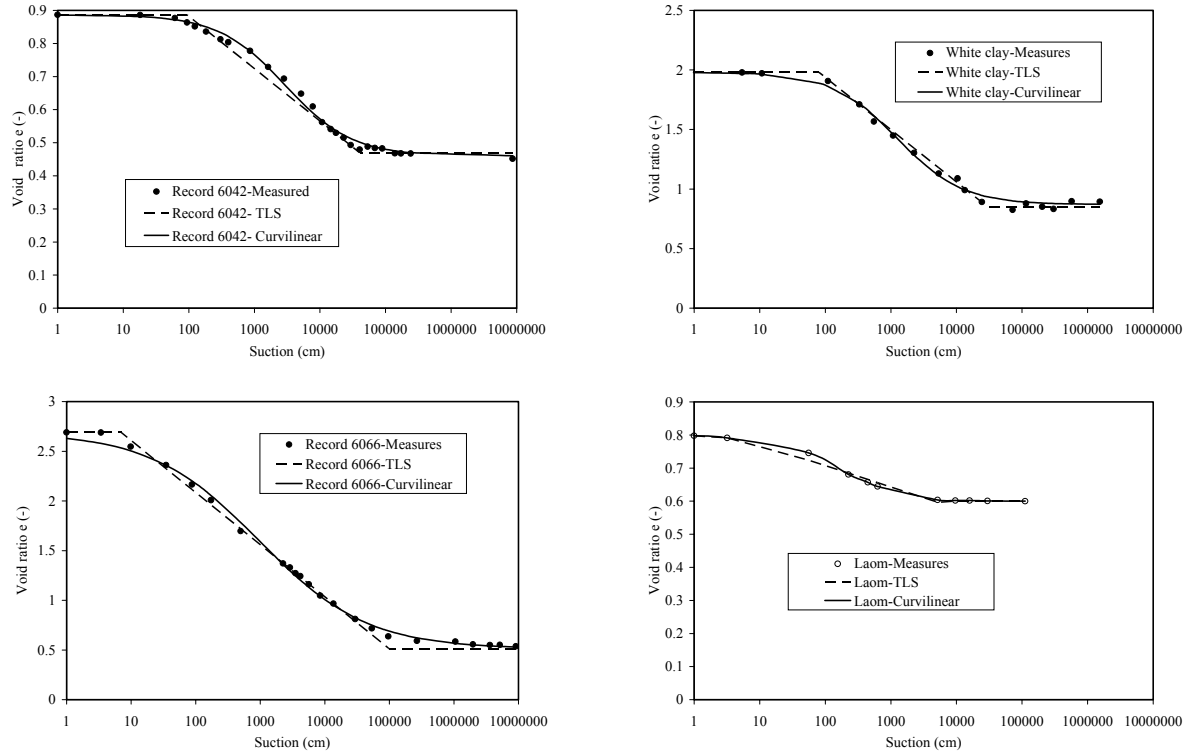


Fig. 3. Typical results for the fitting of measured data using the TLS and curvilinear equations for the VSC

It is worth mentioning here that the void ratio e_s determined on the $e(w)$ curves (with $e_s = D_r w_s / 100$) and $e(\psi)$ curves should theoretically be similar, but that almost negligible differences have been observed, probably due to the data treatment (i.e. $e(\psi)$ calculated from $e(w)$ and $w(\psi)$ for the data taken from SoilVision and obtained by digitizing for the remaining data).

- Parameters ψ_P , ψ_{es-L} and C_ψ in the TLS equation
 The most representative relationships obtained to correlate suction ψ_{es-L} at the shrinkage limit and ψ_P at point P to relevant geotechnical properties are the followings:

$$[6] \quad \psi_{es-L} = 2.5 \times 10^{-5} \frac{\rho_s^{1.46}}{e_s^{1.46}} w_L^{2.12} = 0.6 \frac{w_L^{2.12}}{w_s^{1.46}}$$

$$[7] \quad \psi_P = 14.4 \left(\frac{e_L}{e_0} \right)^{2.79}$$

In eq. 7, e_L represents the void ratio at the liquid limit w_L under saturated state ($e_L = D_r w_L / 100$).

Comparison between ψ_{es-L} and ψ_P determined experimentally and estimated with eq. 6 and 7 shows the scatter of data on Fig. 5 and 6. As will be shown below, these are satisfactory results as other sources of uncertainty prevail when looking at predictive applications.

- Parameter C_ψ defined in the $e-\log \psi$ plane plays a similar role as the compressibility index C_c commonly used in theory of consolidation (in the $e-\log \sigma'$ plane). Several empirical expressions have been proposed to estimate C_c using basic geotechnical properties such as the liquid limit w_L and the initial void ratio e_0 (e.g., Bowles 1984; Sridharan and Nagaraj 2000). Along the same lines, the best estimation of C_ψ (for the available data) was obtained with the following empirical expression (see Figure 7):

$$[8] \quad C_\psi = 0.212 \ln \left(\frac{e_0 - e_s}{e_0} \right) + 0.501$$

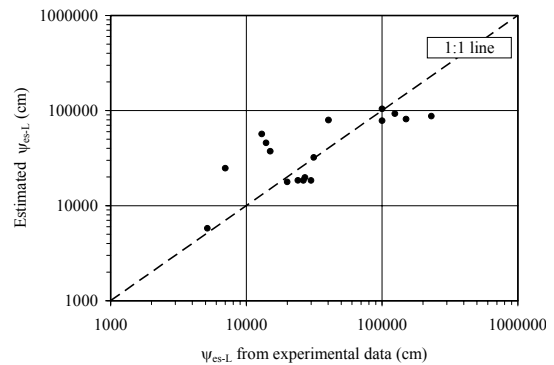


Fig. 5. Comparison between experimental and estimated (eq. 6) values ψ_{es-L} for samples identified in Table 1

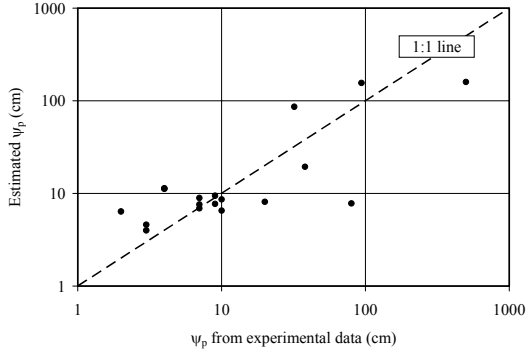


Fig. 6. Comparison between experimental and estimated (with eq. 7) values ψ_P for the samples identified in Table 1

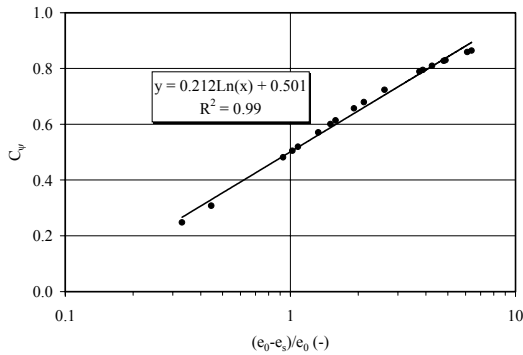


Fig. 7. Empirical relationship used to estimate the shrinkage index C_ψ for the samples identified in Table 1

As e_s depends on w_s , which in turn has been linked to w_L and w_P , C_ψ can also be related to w_L and w_P . Theoretically, $C_\psi = 0$ when $e_0 = e_s$. With the proposed empirical equation, $C_\psi = 0$ when $e_0 \approx 1.1 e_s$; this represents an acceptable deviation for practical applications.

- Parameters α and β in the curvilinear equation

The authors investigation has lead to the following empirical equations to estimate parameters α and β :

$$[9] \quad \alpha = 0.009 \left(\frac{e_L}{e_0} \right)^{-3.1}$$

$$[10] \quad \beta = 0.63 \left(\frac{e_0 - e_s}{e_L} \right)^{-0.22}$$

These relationships confirm that the value of α is inversely proportional to ψ_P (see eq. 7), while that of β can be related to C_ψ (see eq. 8). Parameters α and β determined from the experimental data and estimated using the equations 9 and 10 are compared in Fig. 8 and 9. Although the estimated α and β values are not very accurate for all samples, the results can be considered acceptable for the present preliminary investigations (as will be shown by the VSC predictions made below).

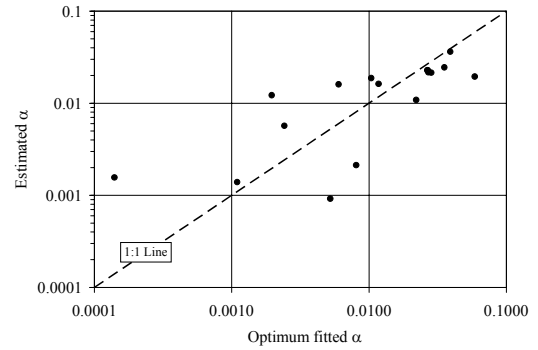


Fig. 8. Comparison between fitted and estimated (with eq. 9) α values for the samples given in Table 1

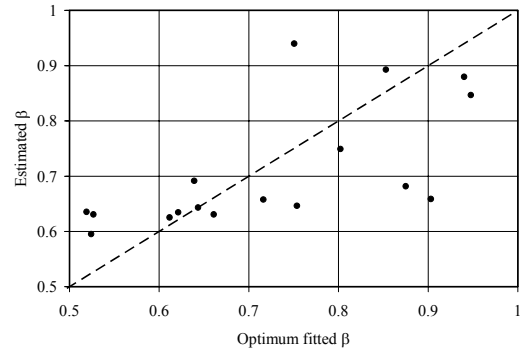


Fig. 9 Comparison between fitted and estimated (with eq. 10) β values for the samples given in Table 1

- Prediction of VSC

The estimation of the parameters for the two models, with the empirical correlations introduced above (equations 5 to 10), can in principle be used to predict the VSC. However, the predictions obtained with the TLS model are still inconclusive, and work is still underway to improve the accuracy of the predictions. This is partly due to imprecision in the definition of parameter C_ψ calculated with eq. 3 using values ψ_{es-L} and ψ_P estimated from eq. 6 and 7; this value of the VSC slope is sometimes quite different than the value C_ψ ensuing from eq. 8. Due to this still unresolved inconsistency, the TSL equations remain in their descriptive format, until more work is done to find the proper solution. At this point, the non linear function (eq. 4) is better suited to predict the VSC, using e_s , α and β derived from eq. 5, 9 and 10 respectively. Measured and predicted VSC are compared in Fig. 10 for some of the data identified in Table 1. The agreement is good in the most cases (Fig. 10a-c), but it can be less satisfactory in a few cases (Fig. 10d). It can be seen that although the correlations for predicting parameters α and β are not very strong, they are adequate to obtain satisfactory predictions of the VSC. These predictions are used in a companion paper to extend the MK model, to estimate the WRC of compressible soil using basic geotechnical properties (Mbonimpa et al. 2005).

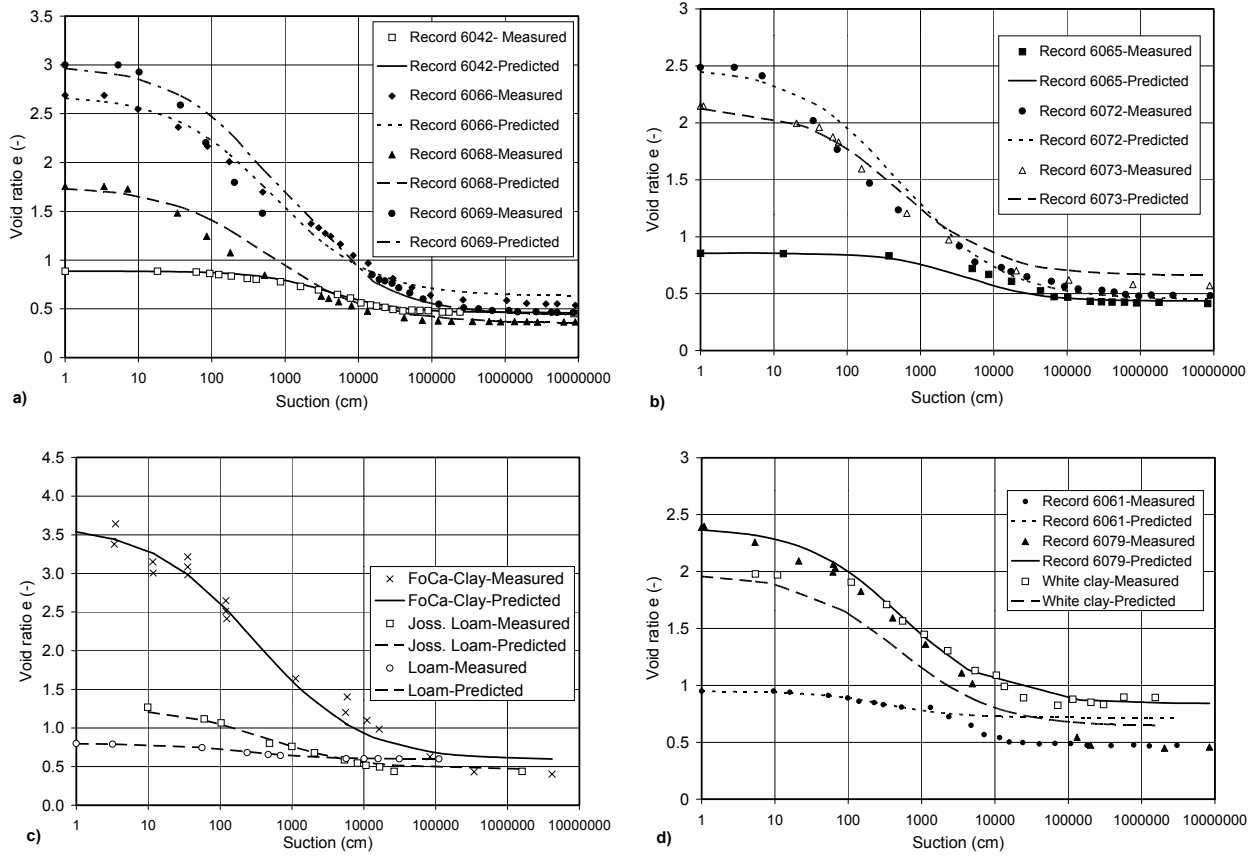


Fig. 10. Typical results for comparisons between measured and predicted VSC

4. DISCUSSION AND CONCLUSION

In this paper, the volumetric shrinkage curve defined by the $e(\psi)$ function has been fitted to a three linear segments (TLS) model (with 3 parameters ψ_P , m_{ψ} , and ψ_{es-L}) and to a continuous curvilinear equation (with 2 parameters α and β). The VSC model parameters obtained from the fitting procedures have been correlated to basic physical soil properties including the initial void ratio e_0 , the solid grain density D_r and the Atterberg (w_L , w_P , w_S) limits. The proposed empirical relationships for the curvilinear model allow predictive applications of the VSC. This constitutes a practical method to estimate the VSC from basic physical properties for soft and initially saturated deformable soils.

The VSC of compressible clayey soils are however governed by many factors including texture, mineralogy, adsorbed cation species, cementing agents, structure and density, stress path and history, etc. (e.g., Marshall et al. 1996; Parker et al. 1997). In the proposed predictive model application, these factors are globally taken into account indirectly, by using the Atterberg (w_L , w_P , w_S) limits. The relationships proposed here for predicting the VSC should thus be used with cautions.

Also, the models presented here have been defined for shrinkage patterns similar to the one shown in Fig. 1, where the saturated (normal) shrinkage follows the saturation line. Results with a structural shrinkage zone or for an initial degree of saturation less than 100% have not been considered; these will be the subject of later studies. Other aspects will also be investigated including the relative contribution of osmotic and matric suction. At the same time, work is also progressing on the suction induced volume change of low plasticity soils such as loose sands, silts and tailings.

More data are necessary for further validation and for developing even more general expressions. A systematic experimental study of undisturbed, compacted, and slurried samples of soils is under way for that purpose.

5. ACKNOWLEDGEMENTS

For this and related projects, the authors received financial support from NSERC and from the participants to the Industrial Polytechnique-UQAT Chair on Environment and Mine Wastes Management (www.polymtl.ca/enviro-geremi).

References

- ASTM D 427-98. 2000. Standard test method for shrinkage factors of soils by the mercury method. Annual handbook of ASTM Standards. ASTM, p. 22-25.
- ASTM D 4943-95. 2000. Standard test method for shrinkage factors of soils by the wax method. Annual handbook of ASTM Standards. ASTM, p. 924-928.
- Aubertin, M., Achib, M., Monzon, M., Joanes, A.M., Bussière, B., and Chapuis, R.P. 1997. Étude en laboratoire sur l'efficacité des barrières de recouvrement construites à partir de résidus miniers. *Rapport de recherche. Projet CDT 1899.3 (version préliminaire décembre 1997 – version finale mars 1999)*. Rapport NEDEM/MEND 2.22.2b, 110 pages.
- Aubertin, M., Mbonimpa, M., Bussière, B., and Chapuis, R.P. 2003. A model to predict the water retention curve from basic geotechnical properties. *Canadian Geotechnical Journal*, 40(6):1104-1122.
- Barbour, S.L. 1998. Nineteenth Canadian Geotechnical Colloquium : The soil-water characteristic curve : a historical perspective. *Canadian Geotechnical Journal*, 35(5), 873-894.
- Biarez, J., Fleureau, J.-M., Zerhouni, M.-I., and Soepandji, B.S. 1987. Variations de volumes des sols argileux lors de cycles de drainage-humidification. *Revue Française de Géotechnique*, 41 : 63-71.
- Bowles, J.E., 1984. *Physical and Geotechnical Soil Properties*. John Wiley & Sons Inc., New York, USA.
- Braudeau, E., and Mohtar, R.H. (2004). Water potential in nonrigid unsaturated soil-water medium. *Water Resources Research*, 40: 1-14.
- Braudeau, E., Costantini, J. M., Bellier, G., and Colleuille, H. 1999. New device and method for soil shrinkage curve measurement and characterisation. *Soil Science Society of America Journal*, 63: 525-535.
- Cabral, A., Planchet, L., Marinho, F.A. and Lefebvre, G. 2004. Determination of the soil water characteristic curve of highly compressible materials. Case study of pulp and paper by-product. *Geotechnical Testing Journal*, 27: 154-162.
- Chertkov V.Y. 2000. Modeling the pore structure and shrinkage curve of soil clay matrix. *Geoderma*, 95: 215-24.
- Chertkov V.Y. 2003. Modelling the shrinkage curve of soil clay pastes. *Geoderma*, 112 : 71-95.
- Crescimanno, G., and Provenzano, G. 1999. Soil shrinkage characteristic curve in clay soils: Measurement and prediction. *Soil Science Society of America Journal*, 63: 25-32.
- Delage, P. and Cui Y.-J. 2000a. L'eau dans les sols non saturés. *Techniques de l'ingénieur, Traité de construction*. Vol. C2, C301-1-19.
- Delage, P. and Cui Y.-J. 2000b. Comportement mécanique des sols non saturés. *Techniques de l'ingénieur, Traité de construction*. Vol. C2, C302-1-19.
- Delleur, J.W. 1999. *The Handbook of Groundwater Engineering*. CRC Press.
- Fleureau, J.-M., Kheirbek-Saoud, S., Soemitro, R., and Taibi, S. 1993. Behaviour of clayey soils on drying-wetting paths. *Canadian Geotechnical Journal*, 30: 287-296.
- Fleureau, J.-M., Verbrugge, J.-C., Huergo, P.J., Correia, A.G., and Kheirbek-Saoud, S. 2002. Aspects of the behaviour of compacted clayey soils on drying and wetting paths. *Canadian Geotechnical Journal*, 39: 1341-1356.
- Fredlund, D.G., and Rahardjo, H. 1993. *Soil Mechanics for Unsaturated Soils*. John Wiley & Sons, Inc., New York, N.Y.
- Fredlund, D.G., and Xing, A. 1994. Equations for the soil-water characteristic curve. *Canadian Geotechnical Journal*, 31(4): 521-532.
- Fredlund, M.D. 1999. SoilVision 2.0, *A knowledge-based database system for unsaturated-saturated soil properties*, Version 2.0n. SoilVision Systems Ltd.
- Gardner W.R. 1956. Calculation of capillary conductivity from pressure plate outflow data. *Soil Science Society of America Journal*, 3: 317-320.
- Geiser, F., Laloui, L., and Vulliet, L. 2000. On the volume measurement in unsaturated triaxial test. *In Unsaturated Soil for Asia*. Edited by H. Rahardjo, D.G. Toll, and E.C. Leong. AA. Balkema, Rotterdam, The Netherland, 669-674
- Haines, W.B. 1993. The volume change associated with variations of water content in soil. *Journal of Agricultural Science*, 13: 296-310.
- Holtz, R.D., and Kovacs W.D. 1981. *An introduction to Geotechnical Engineering*. Prentice-Hall Inc., Englewood Cliffs, N.J.
- Konrad, J.-M., and R. Ayad, R. 1997. An idealized framework for the analysis of cohesive soils undergoing desiccation. *Canadian Geotechnical Journal*, 34: 477-488.
- Marshall, T.J., Holmes, J.W., and Rose, C.W. 1996. *Soil Physics*. Third Edition, Cambridge University Press.
- Mbonimpa, M., Aubertin, M., Bussière, M., Maqoud, A. (2005). A predictive model for the water retention curve of deformable clayey soils. *Journal of Geotechnical and Geoenvironmental Engineering*, ASCE, Submitted
- Parker, J.C., Amos, D.F., and Kaster, D.L. 1977. An evaluation of several methods of estimating soil volume change. *Soil Science Society of America Journal*, 14: 1059-1064
- Ross, J.P., Williams, J., and Bristow, K.L. 1991. Equation for extending water-retention curves to dryness. *Soil Science Society of America Journal*, 5, 923-927.
- Sibley, J.W., and Williams, D.J. 1989. A procedure for determining volumetric shrinkage of an unsaturated soil. *Geotechnical Testing Journal*, 12(3): 181-187.
- Silvestri, V. 1994. Water content relationships of a sensitive clay subjected to cycles of capillary pressures. *Geotechnical Testing Journal*, 17(1): 57-64.
- Sridharan, A., and Nagaraj, H.B. 2000. Compressibility behaviour of remoulded, fine-grained soils and correlation with index properties. *Canadian Geotechnical Journal*, 37(3): 712-722.
- Tripathy, S., Subba Rao, K.S., and Fredlund, D.G. 2002. Water content-void ratio swell-shrink paths of compacted expansive soils. *Canadian Geotechnical Journal*, 39(4): 938-959.
- Wilson, L.G., Everett, L.G., and Cullen, S.J. 2000. *Handbook of Vadose Zone Characterisation and Monitoring*. Lewis Publishers, Boca Raton.